High strain biocompatible polydimethylsiloxane-based conductive graphene and multiwalled carbon nanotube nanocomposite strain sensors

Curtis Lee, Louis Jug, and Ellis Meng[a)]
Department of Biomedical Engineering, University of Southern California, Los Angeles, California 90089-1111, USA

(Received 22 January 2013; accepted 24 April 2013; published online 9 May 2013)

High performance strain sensors were achieved featuring simple, low-cost construction involving the screen printing of combinations of multi-walled carbon nanotube and graphene nano-platelet nanocomposites on biocompatible and flexible polymer substrates. Conductivity and thermal coefficients of resistance of different conductive nanocomposite sensor materials were measured. The zero current resistance and gauge factor of printed sensors was characterized. The combination of high strain operation (up to 40%), high gauge factor (GF > 100), and biocompatible construction pave the way for applications such as minimally invasive *in vivo* strain measurements. © *2013 AIP Publishing LLC*. [http://dx.doi.org/10.1063/1.4804580]

Advances in materials and processing methods, including microcontact printing,[1] oriented nano-wires,[2] "wavy" silicon,[3] and large area reduced graphene oxide,[4] have allowed electronic components (e.g., transistors) to be built on flexible substrates such as polydimethylsiloxane (PDMS), which is a biocompatible, flexible, and transparent polymer that has been shown to be useful for flexible electronics.[5,6] Electronics embedded in or on soft PDMS substrates are now possible by making them thin enough to be flexible,[7] using geometries that allow bending,[6] or incorporating conductive filler material into the PDMS itself.[8]

Carbon nanotubes (CNTs) possess favorable mechanical, thermal, and electrical properties,[9] including intrinsic piezoresistivity resulting in their popularity as a conductive filler material in PDMS-based electronics such as a transistors[8] and strain sensors.[7,10–12] Vacuum filtration[7] and chemical assisted vapor deposition[10] can create thin films of CNTs for transfer onto PDMS. CNTs were also incorporated into PDMS using sonication,[13] shear mixing,[14] magnetic stirring,[15] or by hand[16] to create a conductive PDMS (CPDMS) composite patterned using molds,[11,14] micromolds,[16] or microcontact printing.[12] CNTs are preferred over traditional conductive filler materials such as carbon black and Ag powder because of their low percolation threshold in PDMS (0.2 wt. % to 5 wt. % for carbon nanotubes[8,11] versus 10 wt. % for carbon black and 83 wt. % for 1–2 μm Ag particles[17]).

Graphene is an alternate low cost[18] filler material that has been used with PDMS to form flexible electronics. Graphene shares similar electronic properties as carbon nanotubes[19,20] but is more amenable to patterning and bulk manufacturing through solution based exfoliation,[21] epitaxial growth on metals,[22] or epitaxial decomposition of SiC.[20] Graphene-based flexible strain sensors were realized using a number of techniques to create thin piezoresistive layers. One approach is to deposit graphene on thin layer[23] or 3D matrix[24] of metal (either copper or nikel), encapsulate the layer in PDMS, and then etch away the metal. A layer of graphene platelets was achieved by filtration followed by transfer of the resulting layer onto a polymer substrate.[25] Similarly, a dispersion of graphene oxide platelets was combined with a polymer precursor and reduced *in situ*.[26]

Hybrid CNT + graphene strain sensors were previously reported using vacuum filtration of a dispersion of CNT + graphene to form a conductive layer that was subsequently transferred onto a polymethylmethacrylate (PMMA) substrate.[25] Here, we present hybrid strain sensors featuring a piezoresistive composite made from multiwalled carbon nanotubes (MWNT), graphene nanoplatelets (GNPs), or a combination of the two in a PDMS prepolymer to form a screen printable CPDMS. Piezoresistive CPDMS was sandwiched between PDMS layers to realize flexible strain sensors with high gauge factor and capable of high strain operation. Although piezoresistive composites consisting of CNTs and PDMS were previously reported,[11,15] biological applications were not considered and thus a stiffer PDMS (Sylgard 184) was used. Here, medical grade PDMS (MDX-4-4210, a US Pharmacoepia class VI material) was used to form a nanocomposite sensor material.

The piezoresistivity of CPDMS, useful for strain and other sensing applications, arises primarily from (1) strain-induced break up of conductive networks, (2) the intrinsic piezoresistivity of the filler, and (3) the change in resistance due to electron tunneling, which changes dramatically as a function of filler separation. Simulations indicate that applied strain does not sufficiently disrupt conductive nanonetworks to significantly alter bulk resistance of material,[27] suggesting that the other two mechanisms are responsible. Piezoresistivity contributed by CNTs in conductive composites is dependent on the diameter of tube used. For thicker MWNT tubes having a diameter ~65 nm, there is poor load transfer, and piezoresistivity is dominated by inter tube distance changes during strain.[28] However, for thinner tubes with diameters around 10 nm, the intrinsic piezoresistivity of the tubes become significant.[29] The nanotubes used in the current study were 20–30 nm in diameter, and therefore the intrinsic piezoresistivity of the MWNTs are expected to contribute, but not dominate the overall piezoresistivity of the device. The contribution of electron tunneling is

a)Electronic mail: ellis.meng@usc.edu

dependent on the distribution and geometry of the conductive networks formed by the filler material, which is in large part determined by the matrix material and processing parameters.[30] The electron tunneling effects are expected to dominate at low filler concentrations and under high strain when low density of conductive networks is present.

CPDMS in the present work was created by measuring with a precision scale a predetermined amount of carbon filler material, either GNP and/or MWNT (cheaptubes.com, Brattleboro, VT), and PDMS (MDX4-4210, Factor II, Inc., Lakeside, AZ) base into a glass beaker to create a CPDMS prepolymer. To this was added 10–15 mL of a solvent mixture consisting of a 30:70 ratio of IPA and Stoddard solvent (by volume). The mixture was then placed in an ultrasonic bath (Bransonic 3510, Branson Ultrasonic Corp., Danbury, CT) for 15–18 h to achieve thorough mixing of the filler material with the PDMS base and evaporate the solvent. Using this method, CPDMS base with a range of concentrations of MWNT and GNP were prepared (Fig. 1). Crosslinker (in a ratio of 1:10 to the base) was added to the nanocomposite conductive filler-PDMS base mixture using a planetary mixer (Thinky Corp., Laguna Hills, CA), and the obtained conductive prepolymer was screen printed onto a 500 μm thick layer of non-conductive medical grade PDMS using a lithographically defined brass screen prepared using a previously developed method.[31] Briefly, CPDMS prepolymer was spread across a custom stencil using a plastic squeegee. The stencil was made by etching away a lithographically defined pattern in a 76 μm thick brass shim (4.5 × 6 in.) sandwiched between two sheets of a negative, dry-film photoresist. The photoresist was exposed using a high resolution transparency mask (Mikacolor, Los Angeles, CA) and UV light source (45 mJ/cm^2) and developed in a dilute sodium hydroxide bath. The exposed brass regions were etched away using ferric chloride. The parts for this etching kit were purchased from MicroMark (Berkeley Heights, NJ).

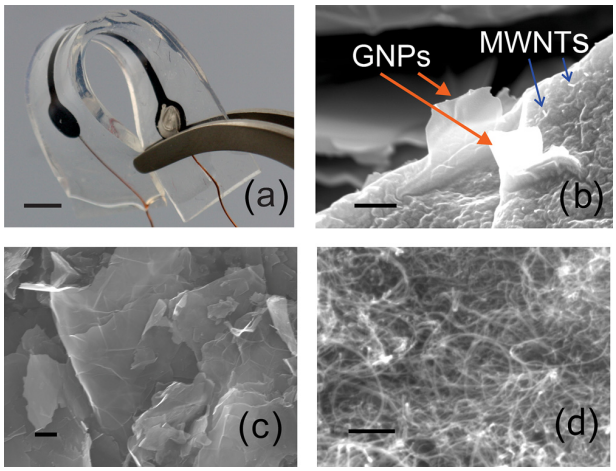

FIG. 1. (a) Photograph of screen-printed MWNT/GNP strain sensor (scale bar is 5 mm). (b) Cross sectional SEM image of strain sensor thick film prepared by freeze fracture (scale bar is 1 μm). GNPs appear as flakes (denoted by orange, thick arrows). MWNTs appear as solid white dots or filaments (denoted by thin blue, arrows). For comparison, (c) GNPs (scale bar is 1 μm) and (d) MWNTs (scale bar is 500 nm) are shown in their pre-processed state.

The screen-printed CPDMS was then placed under a vacuum for 3–4 h to remove any remaining solvent and then cured at 80 °C. A second layer of non-conductive medical grade PDMS was added to fully encapsulate the CPDMS. Robust electrical connections were made by threading fine wires through the contact pads several times or making a connection using conductive epoxy (Microcircuit Silver Type O, Transene Company, Inc., Danvers, MA).

Conductivity is achieved when the concentration of filler is sufficient to form contiguous networks within the non-conductive matrix either by direct contact of filler particles (network formation) and/or by electron tunneling through the polymer between closely spaced particles. This percolation threshold concentration is a function of the uniformity of distribution (which is in turn related to the viscosity of the polymer and the preponderance of aggregation of the filler material),[32] aspect ratio, and degree of curvature of the filler material. Single-walled carbon nanotubes (SWNT) are curved,[28] however, MWNT are relatively straight, and therefore the degree of curvature can be ignored.

Conductivity was calculated from sheet resistance measurements using a four point probe ($R_s = 4.53(V/I)$ when probes have equal spacing, films are <40% of probe spacing, and if the edges of the film are more than four times the spacing of the probes[8,16]). Initially, 35 × 45 mm rectangular patterns of CPDMS were printed onto a non-conductive PDMS substrate to ensure that the edges effects were minimized. However, subsequent four point probe measurements performed directly on un-encapsulated sensors (1.8 × 30 mm) yielded identical resistance values; therefore, four point measurements were later made directly on exposed, unencapsulated sensors.

The percolation threshold was 5 wt. % for MWNT-only and MWNT-GNP composites. The percolation threshold for GNP composites was 12.5 wt. % which can be explained by the smaller aspect ratio of the platelets compared to tubes and is similar to values reported by other groups working with graphene polymer composites.[18] Once the percolation threshold is crossed, traditional percolation theory[33] states that conductivity is related to the concentration of the filler material by the following equation:

$$\sigma_{com} = \sigma_0(\phi - \phi_c)^t \quad \text{for} \quad \phi > \phi_c, \tag{1}$$

where σ_{com} is the conductivity of the composite, σ_0 is the conductivity of the filler material, ϕ is the concentration of filler material, ϕ_c is the concentration of the filler material at the percolation threshold, and t is an empirically determined exponent for each system that is related to the aspect ratio, curvature, and degree of aggregation of the filler material. This exponential trend has been confirmed in literature and agrees with experimental results (Fig. 2). Above concentrations of 13% filler material, the MWNT composites were too viscous to screen print and the GNP composites did not cure.

To evaluate the utility of these nanocomposites for strain sensing applications, the zero current resistance (ZCR), thermal coefficient of resistance, soak test performance, and gauge factor were characterized. Zero current resistance was calculated by recording the resistances of the devices from 1–10 μA using a precision multimeter

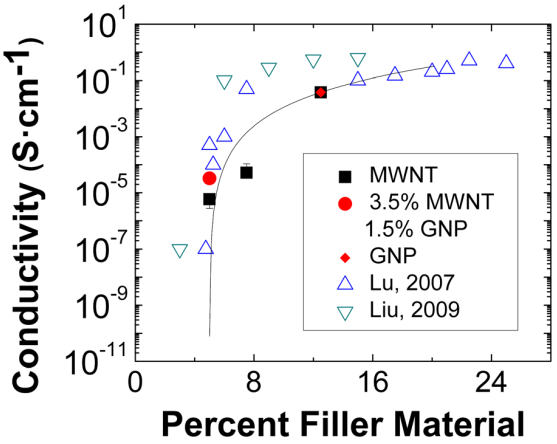

FIG. 2. Conductivity data comparing experimental results against those for similar composites found in literature. Lu *et al.*[11] used 40–60 nm diameter MWNTs and Liu and Choi[12] used 20–40 nm diameter MWNTs.

(Keithley 2400; Keithley Instruments, Cleveland, OH) and extrapolating the resistances back to zero current (Fig. 3(a)). Measuring ZCR in addition to conductivity revealed the current dependency of conductivity which was higher at lower conductivities. The dependency of resistance with current has been suggested in literature to be associated with the increased number of shells contributing to conductance at higher currents in MWNTs[34] and the linear increase in prevalence of electron tunneling with applied voltage.[28,35] The screen printing process allowed three devices to printed at one time and among each batch, the standard error of the ZCR was as low as 3% (data not shown). However, between batches and across different filler concentrations, the standard error of the ZCR was ~20%, with the exception of 69% standard error for the 5% MWNT devices. These data suggest improvements in controlling the thickness of screen printed conductive layers (e.g., automating the process) could reduce the standard error.

The temperature sensitivity of the composite, or temperature coefficient of resistance (TCR), was determined by measuring the device resistance under a constant current bias (10 μA) at different temperatures from 30 to 80 °C (10 °C increments) and taking the slope of the resulting curve (Fig. 3(b)). The TCR for composites made from MWNTs were shown to have a weak dependence on composition and be negative, whereas the TCR for GNP devices were positive. Both of these results are consistent with literature,[36,37] where it is suggested that filler materials with lower aspect ratios (GNPs) will have a positive TCR due to polymeric expansion with temperature that causes increased tunneling resistance which do not affect fillers with high aspect ratios where contact resistance dominates.[37]

Soak testing of strain sensors was performed in 1X PBS (37 °C for 21 days) to simulate *in vivo* conditions and is ongoing (data not shown). Although a decrease in resistance of was observed, likely attributed to penetration of conductive ions into the PDMS, sensors were still operational. It is expected that a thin Parylene coating (few μm) will prevent migration without significantly increasing the stiffness of the sensors.

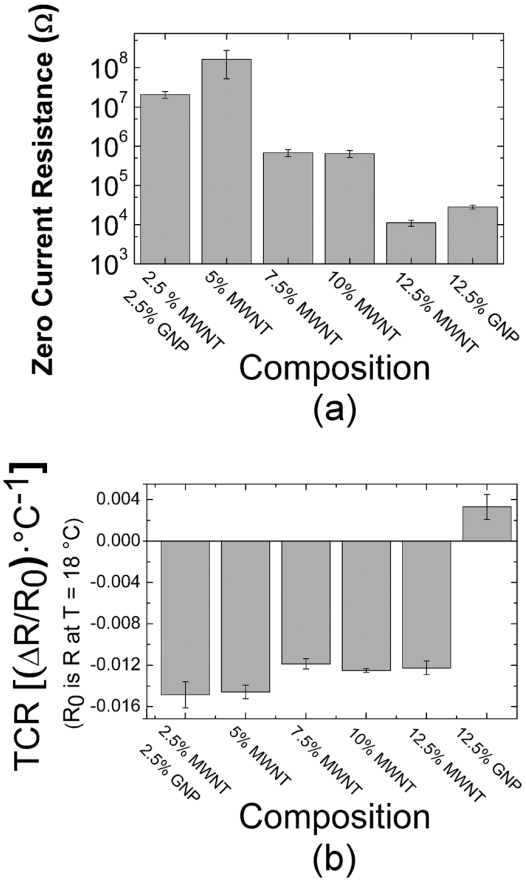

FIG. 3. (a) Zero current resistance (mean ± SE, n = 6–12) and (b) TCR (mean ± SE, n = 3–5).

Gauge factor (*GF*) is a useful measure of merit for piezoresistive strain sensors and is equal to the normalized change in resistance divided by the strain

$$GF = \frac{\frac{\Delta R}{R}}{\frac{\Delta L}{L}} = \frac{\frac{\Delta R}{R}}{\varepsilon}, \tag{2}$$

where R is the nominal as-fabricated, undeformed strain gauge resistance, ΔR is the total change in resistance, L is the original unstrained strain gauge length, ΔL is the change in length following application of strain, and ε is the applied strain. Metal and semiconductors are typical materials used for strain gauges. Metal strain gauges typically have relatively low gauge factors ($GF \sim 2$). Although semiconductors have improved gauge factors ($GF \sim 100$), mechanical properties limit their use to low strain (<0.1%) applications. Thick film materials for strain sensing have reported *GF*s in the range of 2–12.[11,12,38]

Gauge factors of the strain devices were obtained using a motorized stage (Z812; Thorlabs, Newton, NJ) that allowed for user defined strain patterns and a precision multimeter (Keithley 2400; Keithley Instruments, Cleveland, OH). The sensors were mounted to the motorized stage using custom acrylic clamps with a known separation distance and subjected to uniaxial strain using LabVIEW (National Instruments,

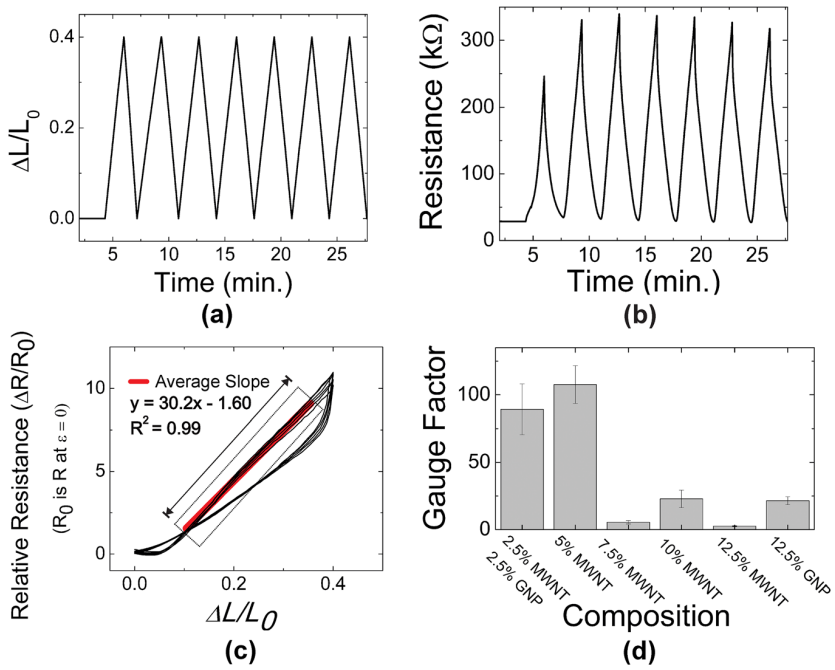

FIG. 4. (a) Strain pattern applied to device. (b) Raw data of resistance versus time. (c) Resistance versus strain (with first 2 cycles removed). Gauge factor obtained by averaging slope of linear region. (d) Gauge factors for various compositions including MWNT and/or GNP fillers (mean ± SE, n = 4–6).

Austin, TX) to control the motor (Figs. 4(a) and 4(b)). Gauge factor was calculated by averaging the linear fit to relative resistance versus uniaxial strain data during the stretching phase of 3–5 strain cycles (Fig. 4(c)) (the R^2 value of the linear regressions ranged from 0.93 to 0.99). Sensors exhibited a "breaking in" cycle, in which the first 1 or 2 cycles had either a higher or lower gauge factor compared to subsequent cycles (Fig. 4(b)), and these cycles were not used when calculating gauge factor. This phenomena is likely due to the differing stiffness between the filler materials and PDMS; the initial strain cycles likely displace some filler relative to the PDMS Two operation regimes were observed: a smaller *GF* at low strain and a larger value at higher strains (Fig. 4(c)). This phenomenon was previously observed in other CNT-polymer composites in which it was hypothesized that at lower strains the change in resistance is dominated by breaking electrical contacts between overlapping CNTs, but at high strain the change in resistance is dominated by increasing the tunneling distance between tubes that are already separated.[39] The present study focused on the device's maximum GF in preparation for high strain biomedical applications, and therefore only the GF at higher strain was calculated.

Gauge factor for our composites ranged from 2 to 22 for high concentrations of filler material (10 wt. % MWNT and 12.5 wt. % GNP) and up to 100 for lower filler concentrations closer to the percolation threshold (5 wt. % MWNT and 3.5 wt. % MWNT + 1.5 wt. % GNP mixture) (Fig. 4(d)). This phenomenon is attributed to the dominance of electron tunneling at filler concentrations close to the percolation threshold; the distance between filler particles increases when the sensors are stretched while still allowing conduction through tunneling. For higher concentrations of filler material, the connections are made mostly by direct contact which are less effected by strain than tunneling electrons. This result is similar to other reported strain sensors made from graphene where it was found that the *GF* was dependent on initial resistance[40] and suggests that high sensitive strain sensors can be made from CPDMS near the percolation threshold of the filler material. The repeatability of *GF* varied based on concentration. Lower filler concentrations were associated with much higher variabilities (standard error values approaching ~20% of the *GF*) whereas the standard error of the *GF* of the higher concentrations were within ~10% of the GF, suggesting that CPDMS at lower concentrations were much more sensitive to processing than higher concentrations.

In summary, strain sensors featuring simple, low-cost construction involving the screen printing of MWNT and GNP nanocomposites on biocompatible medical grade polymer substrates was achieved. The biocompatibility of the substrate, low cost of the GNPs, and strain sensitivity and performance, including high strain operation and gauge factors, of these sensors uniquely enable applications in wearable and implantable sensors in health diagnostics and monitoring.

This work was funded in part by an NSF CAREER Award (ECS-0547544) and the University of Southern California Viterbi Fellowship (CL). The authors would like to thank Dr. Donghai Zhu, Mr. Eric Welder, and the members of the USC Biomedical Microsystems Laboratory for their assistance.

[1]J. S. Brumberg and F. H. Guenther, Expert Rev. Med. Devices **7**(5), 667 (2010).
[2]M. R. Abidian and D. C. Martin, Adv. Funct. Mater. **19**(4), 573 (2009).
[3]D. Lewitus, K. L. Smith, W. Shain, and J. Kohn, Acta Biomater. **7**(6), 2483 (2011); W. He, G. C. McConnell, T. M. Schneider, and R. V. Bellamkonda, Adv. Mater. **19**(21), 3529 (2007).
[4]A. B. Schwartz, Annu. Rev. Neurosci. **27**, 487 (2004).
[5]W. M. Choi, J. Song, D. Y. Khang, H. Jiang, Y. Y. Huang, and J. A. Rogers, Nano Lett. **7**(6), 1655 (2007); D. H. Kim, J. H. Ahn, W. M. Choi, H. S. Kim, T. H. Kim, J. Song, Y. Y. Huang, Z. Liu, C. Lu, and J. A. Rogers, Science **320**(5875), 507 (2008).
[6]D. Y. Khang, H. Jiang, Y. Huang, and J. A. Rogers, Science **311**(5758), 208 (2006).
[7]K. Lee, S. S. Lee, J. A. Lee, K. C. Lee, and S. Ji, Appl. Phys. Lett. **96**(1), 013511 (2010).

[8]C. H. Hu, C. H. Liu, L. Z. Chen, and S. S. Fan, Appl. Phys. Lett. **95**(10), 103103 (2009).
[9]J. H. Du, J. Bai, and H. M. Cheng, Express Polym. Lett. **1**(5), 253 (2007).
[10]T. Yamada, Y. Hayamizu, Y. Yamamoto, Y. Yomogida, A. Izadi-Najafabadi, D. N. Futaba, and K. Hata, Nat. Nanotechnol. **6**(5), 296 (2011).
[11]J. Lu, M. Lu, A. Bermak, and Y. K. Lee, in 7th IEEE Conference on Nanotechnology, Hong-Kong, 2007, p. 1240.
[12]C. X. Liu and J. W. Choi, J. Micromech. Microeng. **19**, 085019 (2009).
[13]M. Lu, A. Bermak, and Y. K. Lee, in 20th IEEE International Conference on Micro Electro Mechanical Systems (IEEE MEMS), Kobe, Japan, 2007, p. 251.
[14]Y. Y. Huang and E. M. Terentjev, Adv. Funct. Mater. **20**(23), 4062 (2010).
[15]C. X. Liu and J. W. Choi, IEEE Trans. Nanotechnol. **9**(5), 590 (2010).
[16]J. Engel, J. Chen, N. Chen, S. Pandya, and C. Liu, in 19th IEEE International Conference on Micro Electro Mechanical Systems (IEEE MEMS), Istanbul, Turkey, 2006, p. 246.
[17]X. Z. Niu, S. L. Peng, L. Y. Liu, W. J. Wen, and P. Sheng, Adv. Mater. **19**(18), 2682 (2007).
[18]S. Stankovich, D. A. Dikin, G. H. B. Dommett, K. M. Kohlhaas, E. J. Zimney, E. A. Stach, R. D. Piner, S. B. T. Nguyen, and R. S. Ruoff, Nature (London) **442**(7100), 282 (2006).
[19]K. S. Novoselov, A. K. Geim, S. V. Morozov, D. Jiang, M. I. K. I. V. Grigorieva, S. V. Dubonos, and A. A. Firsov, Nature (London) **438**(7065), 197 (2005).
[20]C. Berger, Z. Song, T. Li, X. Li, A. Y. Ogbazghi, R. Feng, Z. Dai, A. N. Marchenkov, E. H. Conrad, and N. Phillip, J. Phys. Chem. B **108**(52), 19912 (2004).
[21]D. Li, M. B. Müller, S. Gilje, R. B. Kaner, and G. G. Wallace, Nat. Nanotechnol. **3**(2), 101 (2008).
[22]J. Wintterlin and M. L. Bocquet, Surf. Sci. **603**(10), 1841 (2009).
[23]S.-H. Bae, Y. Lee, B. K. Sharma, H.-J. Lee, J.-H. Kim, and J.-H. Ahn, Carbon **51**(0), 236 (2013).
[24]Z. Chen, W. Ren, L. Gao, B. Liu, S. Pei, and H.-M. Cheng, Nat. Mater. **10**(6), 424 (2011).
[25]S. H. Hwang, H. W. Park, and Y. B. Park, Smart Mater. Struct. **22**(1), 015013 (2013).
[26]Y. Hou, D. Wang, X. M. Zhang, H. Zhao, J. W. Zha, and Z. M. Dang, J. Mater. Chem. C **1**, 515 (2013).
[27]T. C. Theodosiou and D. A. Saravanos, Compos. Sci. Technol. **70**(9), 1312 (2010).
[28]N. Hu, Y. Karube, C. Yan, Z. Masuda, and H. Fukunaga, Acta Mater. **56**(13), 2929 (2008).
[29]G. Yin, N. Hu, Y. Karube, Y. Liu, Y. Li, and H. Fukunaga, J. Composite Mater. **45**(12), 1315 (2011).
[30]N. Hu, Z. Masuda, G. Yamamoto, H. Fukunaga, T. Hashida, and J. Qiu, Composites, Part A **39**(5), 893 (2008).
[31]C. A. Gutierrez and E. Meng, J. Micromech. Microeng. **20**(9), 095028 (2010).
[32]J. O. Aguilar, J. R. Bautista-Quijano, and F. Avilés, Express Polym. Lett. **4**(5), 292 (2010).
[33]G. Deutscher, *in Percolation, Localization, and Superconductivity*, edited by A. M. Goldman and S. A. Wolf (Plenum Press, New York, 1984), p. 95.
[34]R. Hobara, S. Yoshimoto, T. Ikuno, M. Katayama, N. Yamauchi, W. Wongwiriyapan, S. Honda, I. Matsuda, S. Hasegawa, and K. Oura, Jpn. J. Appl. Phys. **43**(8B), L1081 (2004).
[35]J. G. Simmons, J. Appl. Phys. **34**(9), 2581 (1963).
[36]C. Gau, H. S. Ko, and H. T. Chen, Nanotechnology **20**(18), 185503 (2009).
[37]S. Ansari and E. P. Giannelis, J. Polym. Sci., Part B: Polym. Phys. **47**(9), 888 (2009).
[38]P. Giannone and S. Graziani, in Instrumentation and Measurement Technology Conference, 2009, p. 593.
[39]M. Park, H. Kim, and J. P. Youngblood, Nanotechnology **19**(5), 055705 (2008).
[40]J. Zhao, C. He, R. Yang, Z. Shi, M. Cheng, W. Yang, G. Xie, D. Wang, D. Shi, and G. Zhang, Appl. Phys. Lett. **101**(6), 063112 (2012).